# PGRL1 and LHCSR3 Compensate for Each Other in Controlling Photosynthesis and Avoiding Photosystem I Photoinhibition during High Light Acclimation of Chlamydomonas Cells

Frédéric Chaux, Xenie Johnson, Pascaline Auroy, Audrey Beyly-Adriano, Isabelle Te, Stéphan Cuiné, G. Peltier

*Special Issue on the Dynamics of Photosynthesis*

# PGRL1 and LHCSR3 compensate for each other in controlling photosynthesis and avoiding Photosystem I photoinhibition during high light acclimation of *Chlamydomonas* cells

Frédéric Chaux[1], Xenie Johnson[1], Pascaline Auroy[1], Audrey Beyly-Adriano[1], Isabelle Te[1], Stéphan Cuiné[1], Gilles Peltier[1]

[1]CEA, CNRS, Aix-Marseille Université, Institut de Biosciences et Biotechnologies Aix-Marseille, UMR 7265, Laboratoire de Bioénergétique et Biotechnologie des Bactéries et Microalgues, CEA Cadarache, Saint-Paul-lez-Durance, F-13108 France

Corresponding author:
Dr. Gilles Peltier
gilles.peltier@cea.fr

CEA Cadarache
13108 Saint-Paul-lez-Durance
France
+33 4 42 25 76 51
+33 4 42 25 62 65

*Dear Editor*,

In natural environments, photosynthetic organisms experience frequent changes in the light supply, requiring modulation of light harvesting and electron transfer reactions to avoid mismatch between light conversion and metabolic reactions which may result in the production of harmful reactive oxygen species. They have thus evolved photoprotective regulatory mechanisms including the dissipation of excess energy (or non-photochemical quenching, NPQ), which relies on specific light harvesting antennae, such as PSBS and Light-Harvesting Complex Stress-Related 3 (LHCSR3) (Peers et al., 2009), and is triggered by low pH in the thylakoid lumen. The photosynthetic control, which consists of a down-regulation of electron flow between PSII and PSI by the slowing effect of trans-thylakoidal proton gradient on cytochrome $b_6f$ electron transfer, also contributes to photoprotection (Suorsa et al., 2012). Cyclic electron flow around PSI (CEF), that involves Proton Gradient Regulation 5 (PGR5) and PGR5-Like Photosynthetic Phenotype 1 (PGRL1), generates a component of the proton gradient critical for the induction of both NPQ (Munekage et al., 2002) and photosynthetic control (Suorsa et al., 2012; Tolleter et al., 2011). In the present study, we questioned whether NPQ strictly depends on CEF, and whether these two mechanisms may work independently. We also explored to what extent these regulatory mechanisms could limit the maximal capacity of $CO_2$ assimilation and biomass productivity by excessively down-regulating the photosynthetic electron flow, as it was recently reported that biomass productivity was increased in the *C. reinhardtii npq4* mutant (Berteotti et al., 2016).

To answer these questions, we grew *C. reinhardtii pgrl*, *npq4* and *pgrl1npq4* mutant strains in controlled photobioreactors (PBRs) operated as turbidostats and measured $CO_2$ exchange rates and the specific growth rate during a transient from non-saturating light to saturating light under non-limiting $CO_2$ conditions. In this cultivation mode, the cell density of the culture is maintained constant by dilution with fresh medium, thus ensuring a well-controlled light supply. $CO_2$-enriched air was bubbled at a constant flow rate and $CO_2$ concentration was measured in the outflow to determine $CO_2$ uptake rates (Supplemental Figure S1 A,B). Based on $CO_2$ assimilation saturation curves (Supplemental Figure S1C) we selected two light intensities, a non-saturating low light (LL) level (40 µmol photons $m^{-2}$ $s^{-1}$) and a saturating high light (HL) level (200 µmol photons $m^{-2}$ $s^{-1}$) to further investigate on the different *C. reinhardtii* strains during a LL to HL switch (Figure 1A,B). No significant difference in $CO_2$ uptake rates was observed between the four genotypes under LL. Upon transition to HL, $CO_2$ uptake rates increased in a similar manner in the WT and in single

mutants, but dramatically decreased after 2 hours HL in the double *pgrl1npq4* mutant. The $CO_2$ uptake rate thereafter increased in the double mutant and displayed an oscillatory mode indicating the involvement of long-term acclimation mechanisms (Supplemental Figure S2). Similar effects were observed on specific growth rates (Supplemental Figure S3). All four strains showed similar growth rate increases during transition to a lower, non-saturating light intensity (Supplemental Figure S4). The strong inhibition of $CO_2$ uptake observed in the *C. reinhardtii* double *pgrl1npq4* mutant in comparison to the WT upon HL exposure, and the absence of inhibition in single mutants (*pgrl1* or *npq4*), show that PGRL1 and LHCSR3 can compensate for each other in the acclimation of photosynthesis to saturating light. This result obtained in non-limiting $CO_2$ and light conditions is in line with a recent report showing a stronger growth delay in the double mutant *pgrl1npq4* in comparison to single mutants under mixotrophic conditions (Kukuczka et al., 2014), but contrasts with experiments performed under $CO_2$ limitation, in which a strong PSI inhibition was observed in both *pgrl1* (Dang et al., 2014) and *pgrl1npq4* (Bergner et al., 2015) mutants. This suggests that the functional redundancy between PGRL1 and LHCSR3 may be modulated by carbon avaibility.

PSII and PSI measurements were then performed to determine at which level photosynthesis is affected in the double mutant. The maximum PSII yield (ΦPSIImax) measured by chlorophyll fluorescence remained almost constant in the WT, *pgrl1* and *npq4*, while a slight decrease was observed in *pgrl1npq4* (Figure 1C). As expected, NPQ was slightly lower in *pgrl1* than in the WT, but much lower in *npq4* and in *pgrl1npq4* mutants (Supplemental Figure S6). PSI photochemistry, measured as the maximum oxidizable P700, was slightly affected in the WT and in single *pgrl1* and *npq4* mutants, but severely dropped in the double mutant after 4 hours of HL (Figure 1D). Interestingly, the decrease in PSI lagged 1-2 hours after the drop in $CO_2$ uptake (Figure 1G), indicating that PSI inhibition was not the cause, but rather the consequence of the $CO_2$ uptake drop. The decrease in PSI activity was not accompanied by a decrease in PsaA subunit amounts even after 24h (Supplemental Figure S5), indicating that PSI inhibition in *pgrl1npq4* results from an acceptor side limitation rather than from PSI degradation (Chaux et al., 2015). This effect therefore sharply contrasts with previous observations performed under limiting $CO_2$ conditions, in which the PSI activity decrease observed in *pgrl1* or *pgrl1npq4* mutants was accompanied by a decrease in PSI subunit amounts (Bergner et al., 2015; Dang et al., 2014). LHCSR3 was not detected under LL in the WT but transiently accumulated upon exposure to high light, peaking at around 2-4 hours of light exposure (Figure 1E). In *pgrl1*, LHCSR3 was detected in LL and accumulated

in HL to much higher amounts than in the WT. Since the NPQ intensity has been correlated to LHCSR3 accumulation (Bonente et al., 2012), it seems likely that higher LHCSR3 amounts accumulating in *pgrl1* contribute to compensate for the lack of cyclic electron flow. We therefore conclude that LHCSR3 is active in *pgrl1* despite the absence of a proton gradient component generated by cyclic electron flow. The water-water cycle, which is enhanced in *pgrl1* and *pgr5 C. reinhardtii* mutants (Dang et al., 2014; Johnson et al., 2014) may contribute to generate the extra proton gradient needed for the induction of NPQ. On the other hand, PGRL1 accumulated to similar levels in the WT and *npq4* both at LL and HL (Figure 1F), indicating that absence of LHCSR3 is not compensated by increased amounts of PGRL1. Since the rate of PGRL1-CEF is regulated *in vivo* by the redox poise of molecular intermediates (Alric, 2010), it seems likely that up-regulation of CEF activity compensates for the deficiency of thermal dissipation in *npq4* by increasing the photosynthetic control.

In order to better understand the HL-induced inhibition observed on the double mutant, the different strains were then exposed to a slow and gradual (30 hours) increase in light intensity (from 40 to 200 μmol photons $m^{-2}$ $s^{-1}$). A strong decrease of $CO_2$ assimilation was observed in the double mutant, but only when the light intensity reached the saturation level (Supplemental Figure S7). This experiment shows that PSI inhibition in the double mutant does not result from a HL stress effect, but rather results from an inability of the double mutant to maintain a maximal level of photosynthesis under saturating light. Neither the $CO_2$ uptake rate nor the biomass productivity was improved in *pgrl1* and *npq4* mutants in comparison to the WT, showing that none of these mechanisms actually limits biomass productivity under our experimental conditions. This result sharply contrasts with a recent work reporting an increase in biomass productivity in the *C. reinhardtii npq4* mutant in comparison to the WT (Berteotti et al., 2016). Such a contrast is rather intriguing and may be explained by different experimental conditions and set-ups. For instance, our experiments were performed at constant biomass by operating PBRs in the turbidostat mode, whereas the biomass increase was recorded in batch cultures in (Berteotti et al., 2016). Also, our experiments were performed under saturating $CO_2$ concentration and non-limiting light, resulting in a doubling time around 4-5 hours, while $CO_2$ supply was likely limiting in (Berteotti et al., 2016) since air bubbled through PBRs resulted in a much higher doubling time (estimated at around 24 hours).

We conclude from this work that photoprotection can be promoted by LHCSR3 despite the absence of PGRL1 cyclic electron flow, and that PGRL1 and LHCSR3 can work

together or independently and compensate for each other during high light acclimation. The absence of both mechanisms neither improves $CO_2$ uptake nor biomass productivity under non-limiting light and $CO_2$, but compromises both $CO_2$ uptake and biomass productivity. PGRL1 and/or LHCSR3, by contributing to the regulation of electron flow upstream of PSI, limit the accumulation of electrons on the PSI acceptor side, thus avoiding PSI photoinhibition (Supplemental Figure S8).

## SUPPLEMENTAL INFORMATION

Supplemental information is available at *Molecular Plant Online*.


## FUNDING

F.C. was recipient of a Ph.D grant of the CEA Tech Division of the "Commissariat à l'Energie Atomique et aux Energies Alternatives". This work was supported by the "Agence Nationale pour la Recherche" ChloroPaths project (ANR-14-CE05-0041-01) and the A*MIDEX (ANR-11-IDEX-0001-02) project. Experimental support was provided by the HélioBiotec platform, funded by the European Union (European Regional Development Fund), the Région Provence Alpes Côte d'Azur, the French Ministry of Research and the CEA.


## AUTHOR CONTRIBUTIONS

F.C., X.J. and G.P. designed the research. F.C, S.C., P.A., A.B-A., and I.T. performed the experiments. F.C., X.J. and G.P. interpreted the data and wrote the manuscript.


## ACKNOWLEDGMENTS

We thank Pierre-Louis Lucas for technical support, Pr. Michael Hippler (IBBP, WWU Munster, Germany) for the kind supply of *pgrl1npq4* strain, Dr. Jean Alric for fruitful discussions, and Léo Dubus for improvement of PBR-monitoring software. No conflict of interest declared.

LEGEND OF FIGURE

**Figure 1. Time course of $CO_2$ uptake and specific growth rates measured in *Chlamydomonas* wild-type cells and in *pgrl*, *npq4* and *pgrl1npq4* mutants during a rapid transition from LL to HL.** Cells were grown photoautotrophically in PBRs operated as turbidostats in the presence of 1.8% $CO_2$ in air under non-saturating light (LL, 40 µmol photons $m^{-2}$ $s^{-1}$). After at least 24 hours stabilization under LL, light intensity was suddenly increased to 200 µmol photons $m^{-2}$ $s^{-1}$ (HL). (A) Representative measurements of $CO_2$ uptake rates performed on a set of 4 PBRs. (B) Means values (± SD) from 3 biological replicates of $CO_2$ uptake (left panel) and specific growth rates (right panel) measured under LL, and upon 1 hour or 4 hours HL exposure. Differences between strains were not significant (t-test, $p$>0.05), except for the *pgrl1npq4* after 4 hours HL. (C, D, E, F, G) At different time points, aliquots were harvested from PBR cultures for PSII, PSI measurements and immuno-detection analysis. (C) Maximal PSII yield was measured after 5 min dark acclimation as $(F_M-F_0)/F_M$. Shown are mean values (± SD, n=3). (D, G) PSI activity was measured as the oxidizable P700 content calculated from light-minus-dark absorbance difference at 705nm in the presence of DCMU and methylviologen. Shown (D) are mean values (± SD, n=3) for LL and after 8 hours HL measurements. (E) LHCSR3 and (F) PGRL1 protein accumulation in *C. reinhardtii* wild-type and *pgrl1*, *npq4* and *pgrl1npq4* mutant strains upon a LL to HL transient. Samples were loaded at equal total proteins amounts based on Coomassie blue staining (Control). (G) $CO_2$ uptake rates (closed symbols) and maximum oxidizable P700 content (open symbols) measured during a LL to HL transient in three independent *pgrl1npq4* strains.

LITERATURE CITED

**Alric, J.** (2010). Cyclic electron flow around photosystem I in unicellular green algae. Photosynth. Res. **106**:47-56.

**Bergner, S.V., Scholz, M., Trompelt, K., Barth, J., Gabelein, P., Steinbeck, J., Xue, H., Clowez, S., Fucile, G., Goldschmidt-Clermont, M., et al.** (2015). STATE TRANSITION7-dependent phosphorylation is modulated by changing environmental conditions, and Its absence triggers remodeling of photosynthetic protein complexes. Plant Physiol. **168**:615-634.

**Berteotti, S., Ballottari, M., and Bassi, R.** (2016). Increased biomass productivity in green algae by tuning non-photochemical quenching. Sci. Rep. **6**.

**Bonente, G., Pippa, S., Castellano, S., Bassi, R., and Ballottari, M.** (2012). Acclimation of *Chlamydomonas reinhardtii* to different growth irradiances. J. Biol. Chem. **287**:5833-5847.

**Chaux, F., Peltier, G., and Johnson, X.** (2015). A security network in PSI photoprotection: regulation of photosynthetic control, NPQ and O2 photoreduction by cyclic electron flow. Front. Plant Sci. **6**:875.

**Dang, K.V., Plet, J., Tolleter, D., Jokel, M., Cuine, S., Carrier, P., Auroy, P., Richaud, P., Johnson, X., Alric, J., et al.** (2014). Combined increases in mitochondrial cooperation and oxygen photoreduction compensate for deficiency in cyclic electron flow in *Chlamydomonas reinhardtii*. Plant Cell **26**:3036-3050.

**Johnson, X., Steinbeck, J., Dent, R.M., Takahashi, H., Richaud, P., Ozawa, S., Houille-Vernes, L., Petroutsos, D., Rappaport, F., Grossman, A.R., et al.** (2014). Proton gradient regulation 5-mediated cyclic electron flow under ATP- or redox-limited conditions: a study of DeltaATPase *pgr5* and DeltarbcL *pgr5* mutants in the green alga *Chlamydomonas reinhardtii*. Plant Physiol. **165**:438-452.

**Kukuczka, B., Magneschi, L., Petroutsos, D., Steinbeck, J., Bald, T., Powikrowska, M., Fufezan, C., Finazzi, G., and Hippler, M.** (2014). Proton Gradient Regulation5-Like1-mediated cyclic electron flow is crucial for acclimation to anoxia and complementary to nonphotochemical quenching in stress adaptation. Plant Physiol. **165**:1604-1617.

**Munekage, Y., Hojo, M., Meurer, J., Endo, T., Tasaka, M., and Shikanai, T.** (2002). PGR5 is involved in cyclic electron flow around photosystem I and is essential for photoprotection in Arabidopsis. Cell **110**:361-371.

**Peers, G., Truong, T.B., Ostendorf, E., Busch, A., Elrad, D., Grossman, A.R., Hippler, M., and Niyogi, K.K.** (2009). An ancient light-harvesting protein is critical for the regulation of algal photosynthesis. Nature **462**:518-521.

**Suorsa, M., Jarvi, S., Grieco, M., Nurmi, M., Pietrzykowska, M., Rantala, M., Kangasjarvi, S., Paakkarinen, V., Tikkanen, M., Jansson, S., et al.** (2012). PROTON GRADIENT REGULATION5 is essential for proper acclimation of Arabidopsis photosystem I to naturally and artificially fluctuating light conditions. Plant Cell **24**:2934-2948.

**Tolleter, D., Ghysels, B., Alric, J., Petroutsos, D., Tolstygina, I., Krawietz, D., Happe, T., Auroy, P., Adriano, J.M., Beyly, A., et al.** (2011). Control of hydrogen photoproduction by the proton gradient generated by cyclic electron flow in *Chlamydomonas reinhardtii*. Plant Cell **23**:2619-2630.

# Figure 1

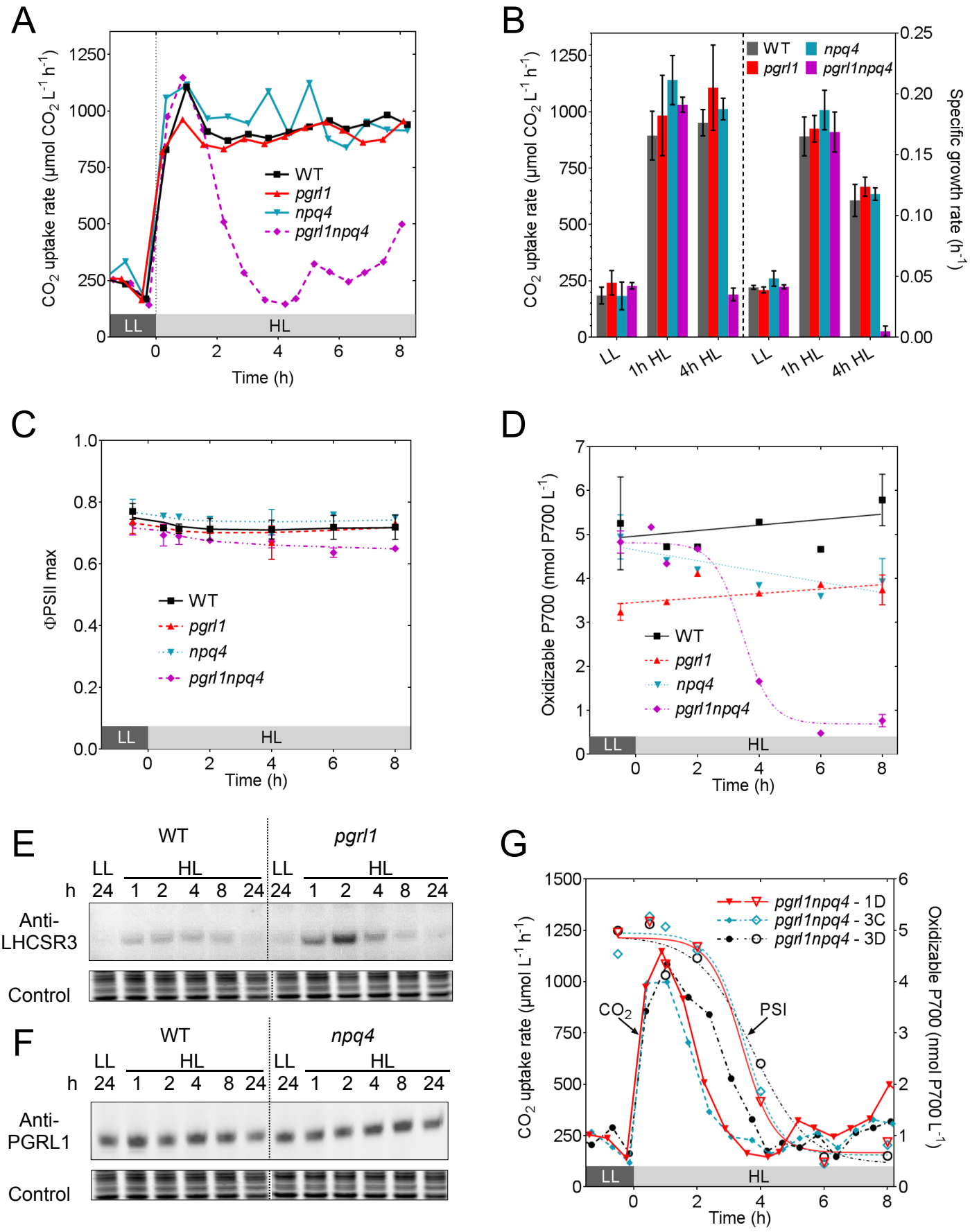
A
CO2 uptake rate (µmol CO2 L-1 h-1)
Time (h)
WT
pgrl1
npq4
pgrl1npq4
LL
HL
B
CO2 uptake rate (µmol CO2 L-1 h-1)
Specific growth rate (h-1)
WT
pgrl1
npq4
pgrl1npq4
LL
1h HL
4h HL
C
ΦPSII max
Time (h)
D
Oxidizable P700 (nmol P700 L-1)
Time (h)
E
WT
pgrl1
h
Anti-LHCSR3
Control
F
WT
npq4
Anti-PGRL1
Control
G
CO2 uptake rate (µmol L-1 h-1)
Oxidizable P700 (nmol P700 L-1)
pgrl1npq4 - 1D
pgrl1npq4 - 3C
pgrl1npq4 - 3D
CO2
PSI
Time (h)

# Supplemental Information

## PGRL1 and LHCSR3 can compensate for each other in controlling photosynthesis and avoiding Photosystem I photoinhibition during high light exposure of Chlamydomonas cells

Frédéric Chaux, Xenie Johnson, Pascaline Auroy, Audrey Beyly-Adriano, Isabelle Te, Stéphan Cuiné, Gilles Peltier

### Materials and Methods

**Strains.** *C. reinhardtii pgrl1* and *npq4* mutants have been previously described (Peers et al., 2009; Tolleter et al., 2011). The *pgrl1npq4* double mutant was generated by serial backcrosses (Kukuczka et al., 2014). Reference wild-type strains (WT) CC-124 (*mt- nit1 nit2*) and CC-125 (*mt+ nit1 nit2*) (Harris, 1989) were obtained from http://www.chlamycollection.org/. A set of double *pgrl1npq4* mutants was generated by standard crossing procedure in our lab and used in some experiments as independent lines (Figures 1, S2 and S6).

**Photobioreactors (PBRs) experiments.** Cells were photoautotrophically cultivated in 1L-photobioreactors (PBR) operated in the turbidostatic mode. Biomass concentration was measured as turbidity ($OD_{880nmn}$) and kept at a constant value by step-wise addition of fresh medium at a constant culture volume. Temperature was controlled at 20°C by and the pH was maintained at a constant value (pH 6.4) by automated addition of 1 M KOH. Light was provided from eight fluorescent tubes (OSRAM DULUX L18W 954, Germany) radially disposed around the PBR, and light levels were measured inside the culture vessel by placing the quantum sensor (LI-189, LI-COR Biosciences, USA) in contact to the vessel. Cultures were continuously bubbled with $CO_2$-enriched air (1.8% $CO_2$ in air) delivered at a constant flow rate (0.5 L $min^{-1}$) by means of four mass flow meters (EL-flow, Bronkhorst High Tech BV, The Netherlands). $CO_2$ concentration was measured in the gas outflow by infrared spectroscopy using a $CO_2$ gas analyzer (LI-840A, LI-COR, USA). An automatically controlled gas chromatography valve (Cheminert C25F, VALCO Instruments Inc. Co., the

USA) was used to sequentially analyze the $CO_2$ concentration of the gas outflow of each PBR. $CO_2$ measurements were performed on a 5 min period for each PBR, so that measurements on a given PBR were performed every 20 min. For accurate $CO_2$ uptake calculation, one of the PBRs was kept cell-free and served as a $CO_2$ control for the three other PBRs. $CO_2$ uptake rates (µmol $CO_2$ $h^{-1}$ $L^{-1}$) were calculated as:

$$CO_2\ uptake\ rate = \frac{1}{V_{PBR}}([CO_2]_{NO\ CELL} - [CO_2]_{CELLS}) * \frac{D_V}{v_M}$$

where $V_{PBR}$ is the volume of the PBR (1 L), $[CO_2]$ is the molar content (ppm) of carbon in the gas from the reference PBR ($_{NO\ CELL}$) or from the cultured ones ($_{CELLS}$), $D_V$ the volumetric flow rate (30 L $h^{-1}$) and $v_M$ the molar volume (24.055 L $mol^{-1}$ at atmospheric pressure and 20°C). Specific growth rates ($h^{-1}$) were calculated as dilution rates (averaged on 10 min period of time) multiplied by the PBR volume (1L).

**Chlorophyll fluorescence measurements.** Cells grown in PBRs were quickly harvested into a glass cuvette and introduced in pulse amplitude modulated fluorimeter (Dual PAM-100, Walz, Germany) where it was continuously stirred to avoid sedimentation. Detection light is blue and very weak (~10 µmol photons $m^{-2}$ $s^{-1}$) while actinic light is red and its level (photosynthetically active radiation, PAR) was adjusted as follows. After 10 min in the dark, basal fluorescence ($F_0$) and maximal fluorescence ($F_M$) were measured in absence of actinic light. Actinic light was switched on to 500 µmol photons $m^{-2}$ $s^{-1}$ for 5 minutes (steady state fluorescence, F) and a saturating flash (6,000 µmol photons $m^{-2}$ $s^{-1}$ during 600 ms) was superimposed every minute ($F_M$'). NPQ values was determined from chlorophyll fluorescence measurements as ($F_M$-$F_M$')/$F_M$'as ($F_M$-$F_M$')/$F_M$' upon 4 min of high light exposure (490 µmol photons $m^{-2}$ $s^{-1}$).

**Absorption change measurements.** Cell suspensions were harvested from PBRs cultures, centrifuged at 3,000 rpm for 2 min and resuspended in 3 mL 20% Ficoll buffered with 20 mM HEPES (pH 7.2). PSII was inhibited by adding 3-(3,4-dichlorophenyl)-1,1-dimethylurea (DCMU) at a 10 µM final concentration. P700 absorption was measured at 705 nm using a JTS-10 (BioLogic, France). Measurements were carried our in the dark to reach a baseline level and under saturating light (1,170 µmol photons $m^{-2}$ $s^{-1}$) where $P700^+$ was accumulated within 1s and represented the total amount of oxidizable P700. Concentration of oxidizable P700 was calculated from steady-state (~5 s) relative absorbance levels and molar extinction coefficient: ($A_{light}$-$A_{dark}$)/( -50 * 2,3 * 5) (Hiyama and Ke, 1972; Joliot and Joliot, 2005). P700

absorption changes were also measured in the presence of the PSI electron acceptor methylviologen (MV) at final concentration 10 mM and in the presence of 10 μM DCMU with similar results similar to that obtained with DCMU alone (not shown).

**Immunodetection.** Cells were harvested from PBR cultures, centrifuged at 3,200 *g* for 2 min, frozen in liquid nitrogen then stored at -20°C until use. Protein samples were prepared as in (Dang et al., 2014) and loaded on one large 10% PAGE Bis-Tris SDS gel buffered with MOPS (pH 7.7). Protein contents were estimated from Coomassie blue staining using an Odyssey IR Imager (LICOR, USA) in order to load equal protein amounts for immunoblot analysis. Proteins were transferred to nitrocellulose membranes by semi-dry transfer (Biorad, CA, USA). Membranes were blocked in milk for at least 30 min and the primary antibody added according to supplier recommendation (Agrisera, Sweden). As an exception, LHCSR3 was detected after dry i-Blot transfer (Thermofischer, MA USA). After 4°C overnight incubation, primary antibody was removed by several rinsing in TBS and a peroxidase-coupled secondary antibody was added for at least 1 hour before detection with a Gbox imaging system (Syngene, UK).

**Statistics.** Statistical analyses were performed with GraphPad Prism software (La Jolla (CA), USA) using t-test with fewer assumptions (consistent SD not assumed). Outcomes were equal whether data where corrected for multiple comparisons using the Holm-Sidak method (recommended) or not. Error bars on graph account for standard deviation. In Figure 1D, linear regression was drawn for the WT and simple *pgrl1* and *npq4* mutants whereas sigmoidal function was fitted to *pgrl1npq4* dataset. Values were fitted as well to sigmoidal functions for *pgrl1npq4* in Figure 1G.

## Supplemental Literature Cited

**Dang, K.V., Plet, J., Tolleter, D., Jokel, M., Cuine, S., Carrier, P., Auroy, P., Richaud, P., Johnson, X., Alric, J., et al.** (2014). Combined increases in mitochondrial cooperation and oxygen photoreduction compensate for deficiency in cyclic electron flow in *Chlamydomonas reinhardtii*. Plant Cell **26**:3036-3050.

**Hiyama, T., and Ke, B.** (1972). Difference spectra and extinction coefficients of P 700. Biochim. Biophys. Acta **267**:160-171.

**Joliot, P., and Joliot, A.** (2005). Quantification of cyclic and linear flows in plants. Proc. Natl. Acad. Sci. USA **102**:4913-4918.

**Kukuczka, B., Magneschi, L., Petroutsos, D., Steinbeck, J., Bald, T., Powikrowska, M., Fufezan, C., Finazzi, G., and Hippler, M.** (2014). Proton Gradient Regulation5-Like1-mediated cyclic electron flow is crucial for acclimation to anoxia and complementary to nonphotochemical quenching in stress adaptation. Plant Physiol. **165**:1604-1617.

**Peers, G., Truong, T.B., Ostendorf, E., Busch, A., Elrad, D., Grossman, A.R., Hippler, M., and Niyogi, K.K.** (2009). An ancient light-harvesting protein is critical for the regulation of algal photosynthesis. Nature **462**:518-521.

**Tolleter, D., Ghysels, B., Alric, J., Petroutsos, D., Tolstygina, I., Krawietz, D., Happe, T., Auroy, P., Adriano, J.M., Beyly, A., et al.** (2011). Control of hydrogen photoproduction by the proton gradient generated by cyclic electron flow in *Chlamydomonas reinhardtii*. Plant Cell **23**:2619-2630.

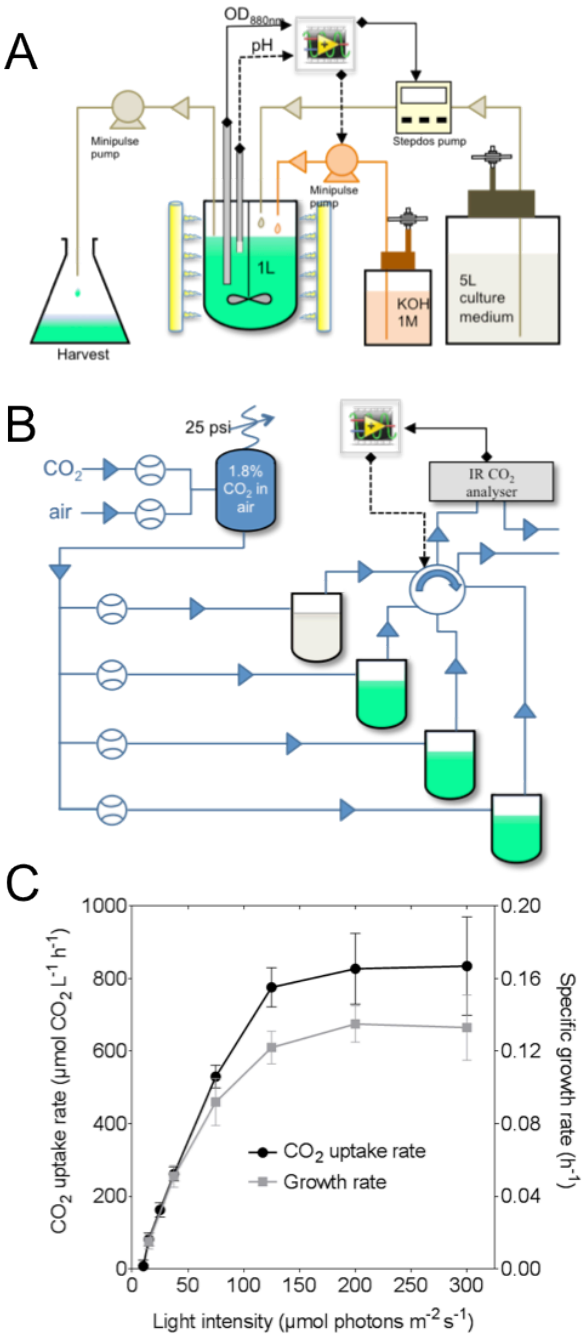


**Supplemental Figure S1. Photobioreactor set-up used to monitor $CO_2$ uptake rates and biomass productivity during steady state growth in microalgae.** (A) Microalgae were grown photoautotrophically in 1L cylindrical photobioreactors radially illuminated and bubbled with $CO_2$-enriched (1.8%) air. Biomass concentration was followed by turbidity measurements ($OD_{880nm}$ = 0.4) and kept at constant level by stepwise dilution by fresh minimal medium. The pH was maintained at a constant value (pH 6.4) by automated addition of 1M KOH. (B) The $CO_2$/air mixture (1.8% in air) was delivered at a constant flow rate (30 L $h^{-1}$) by means of mass flow meters. Outflows from each culture were sequentially analyzed by an infra-red $CO_2$ analyzer. One of the PBRs was run without cells (in grey) and served as a reference value for $CO_2$ consumption measurements in the three cell-containing PBRs (in green). (C) Wild-type *C. reinhardtii* cells were grown under various light intensities. Upon at least 24 hours of stabilization at each light level, $CO_2$ concentrations and dilution rates were measured. Shown are means ± SD (n=3).

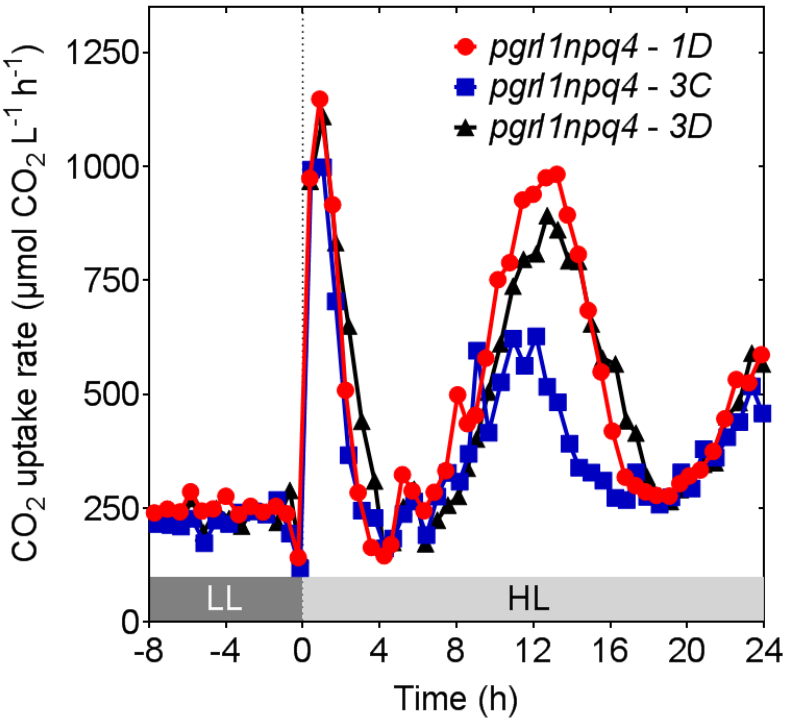


**Supplemental Figure S2. Time course of $CO_2$ uptake rates measured in *pgrl1npq4 C. reinhardtii* cells during a LL to HL transient.** $CO_2$ uptake measurements were performed in three independent *pgrl1npq4* strains as described in Figure 1 and plotted here on a 24 hour period, with t0 corresponding to the light increase (dotted vertical line).

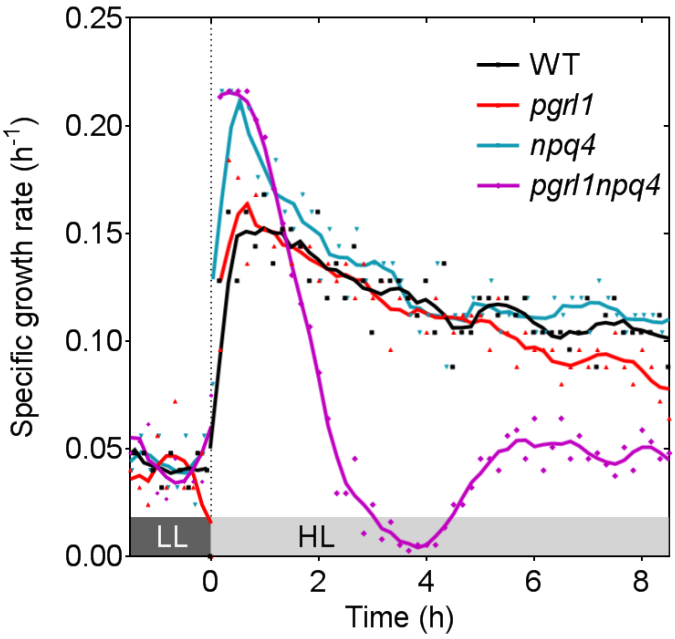


**Supplemental Figure S3. Time course of specific growth rates measured in WT, *pgrl*, *npq4* and *pgrl1npq4 C. reinhardtii* cells during a LL to HL transient.** Cells were grown photoautotrophically in PBRs operated as turbidostats in the presence of 1.8% $CO_2$ in air under non-saturating LL (40 µmol photons $m^{-2}$ $s^{-1}$). After at least 24 hours stabilization, the light intensity was increased to 200 µmol photons $m^{-2}$ $s^{-1}$. Specific growth rates were averaged over 10 min, with t0 corresponding to the light increase (dotted vertical line).

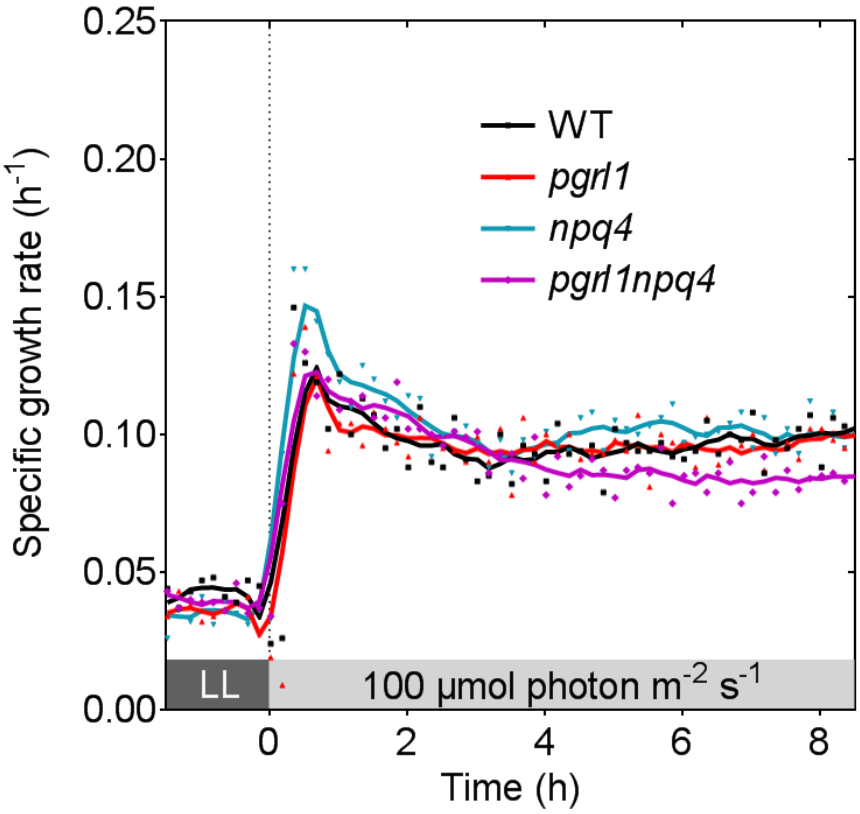


**Supplemental Figure S4. Time course of growth rates measured in WT, *pgrl*, *npq4* and *pgrl1npq4* *C. reinhardtii* cells during a LL to HL transient.** Cells were grown photoautotrophically in PBRs operated as turbidostats in the presence of 1.8% $CO_2$ in air under non-saturating LL (40 µmol photons $m^{-2}$ $s^{-1}$). After at least 24 hours stabilization, the light intensity was increased to 100 µmol photons $m^{-2}$ $s^{-1}$. Specific growth rates were averaged over 10 min, with t0 corresponding to the light increase (dotted vertical line).

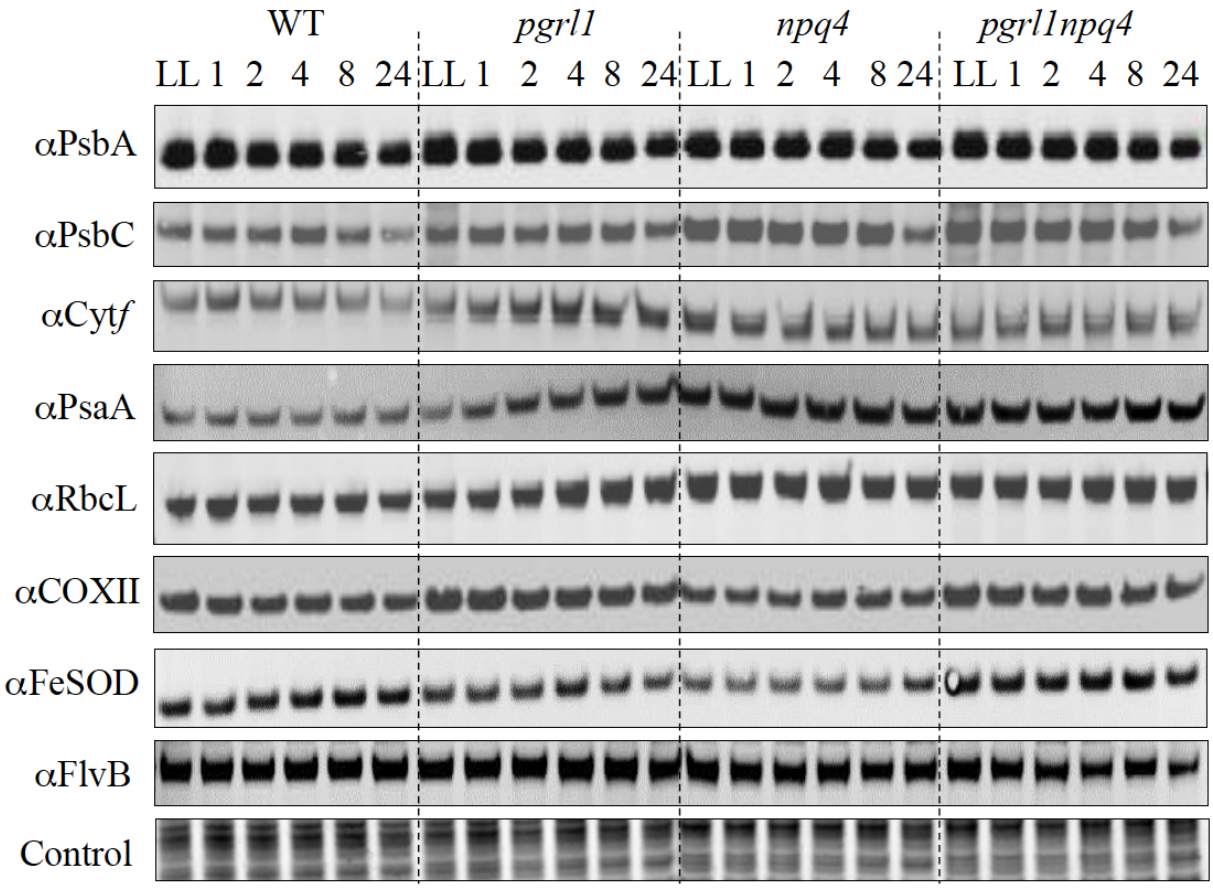


**Supplemental Figure S5. Immunoanalysis of photosynthetic and respiratory protein complexes in wild-type and *pgrl1*, *npq4* and *pgrl1npq4* mutant strains during a LL to HL transient.** Wild-type (WT) and mutant strains were grown in PBRs as described in Figure 1. At the indicated time points, cells were harvested by centrifugation to prepare protein extracts used for immunodetection. Different antibodies raised against PsbA (PSII), PsbC (PSII), Cyt*f,* PsaA (PSI), RbcL (Rubisco), COXIIb (COXII), FeSOD, and FLVB were used to decorate immunoblots. Samples were loaded at equal total proteins amounts based on Coomassie blue staining (Control).

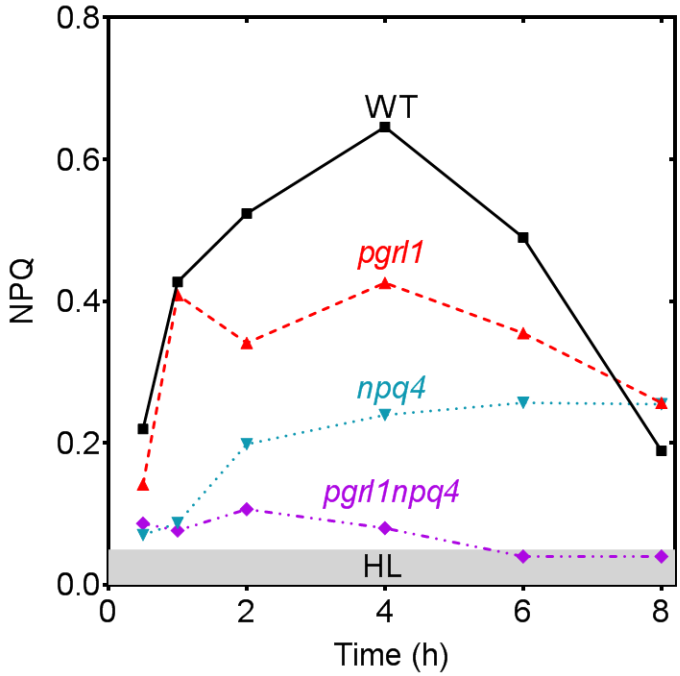


**Supplemental Figure S6. Time course of NPQ measured in WT, *pgrl*, *npq4* and *pgrl1npq4 C. reinhardtii* cells in response to HL exposure.** Wild-type (WT) and mutant strains were grown in PBRs as described in Figure 1. Samples were harvested and stirred in the dark for 10 min. NPQ was then determined upon 4 min of high light exposure (490 µmol photons $m^{-2}$ $s^{-1}$) from chlorophyll fluorescence measurements as $(F_M-F_M')/F_M'$. Shown are NPQ values measured in a representative experiment out of 3 independent experiments for the WT and the *pgrl1npq4* double mutant and of two independent experiments for *pgrl1*, npq4 single mutants, all experiments showing similar tendency.

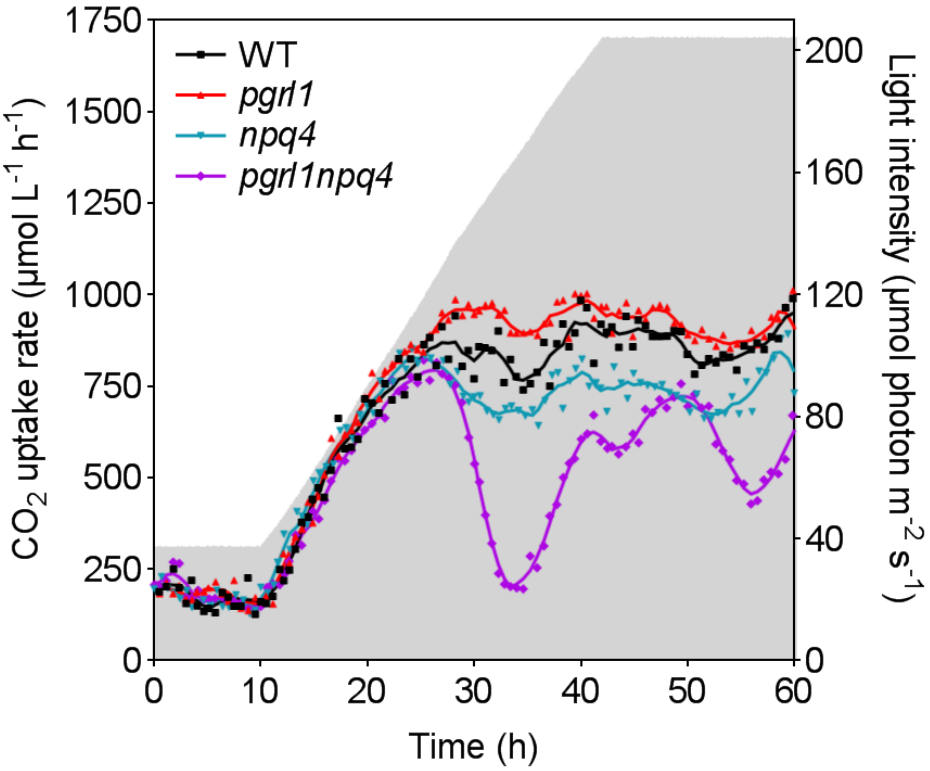


**Supplemental Figure S7. Time course of $CO_2$ uptake rate during a gradual increase from LL to HL in wild-type, *pgrl1*, *npq4* and *pgrl1npq4* *C. reinhardtii* cells grown in photobioreactors.** Wild-type (WT) and mutant strains were grown under LL (40 µmol photons $m^{-2}$ $s^{-1}$) in PBRs operated as turbidostats until a steady-state dilution rate was reached and then maintained for at least 24 hours. Light intensity was then slowly raised during a 30 hours period until reaching a HL intensity (200 µmol photons $m^{-2}$ $s^{-1}$). The gradual increase in light intensity is represented by the grey shaded area.

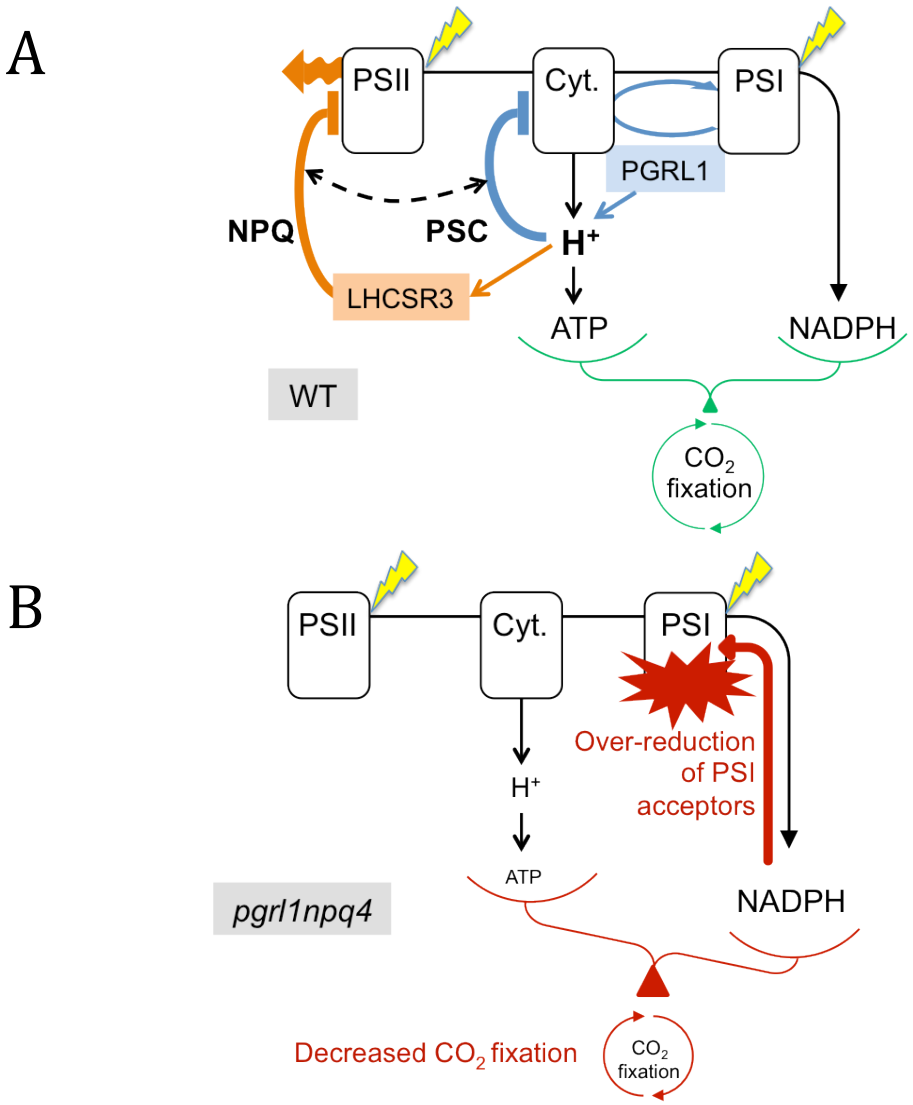


**Supplemental Figure S8. Schematic view of the interplay between PGRL1 and LHCSR3 upon high light exposure and detrimental effect on PSI in the absence of both mechanisms.** (A) Upon high light exposure of WT cells, the proton gradient induces accumulation of LHCSR3 and dissipation of excess energy by NPQ; PGRL1 generates an additional component of the proton gradient that triggers the photosynthetic control (PSC). Both PGRL1 and LHCSR3 participate in maintaining a balanced production of ATP and NADPH, required for optimal $CO_2$ fixation rate; both mechanisms compensate for each other in single *pgrl1* or *npq4* mutants (shown by the dotted arrow). (B) In the double *pgrl1npq4* mutant, the electron flow is no longer controlled under high light neither by PGRL1 nor by LHCSR3; this gradually leads to an increase of the NADPH/ATP balance, which slows down $CO_2$ fixation and in turn leads to PSI photodamage.